Taylor & Francis
Taylor & Francis Group

Fullerenes, Nanotubes and Carbon Nanostructures

ISSN: 1536-383X (Print) 1536-4046 (Online) Journal homepage: www.tandfonline.com/journals/lfnn20

A facile method for fabrication of large area graphene nanostructures

Cihan Kuru & Sungho Jin

To cite this article: Cihan Kuru & Sungho Jin (2017) A facile method for fabrication of large area graphene nanostructures, Fullerenes, Nanotubes and Carbon Nanostructures, 25:11, 642-645, DOI: 10.1080/1536383X.2017.1373097

To link to this article: https://doi.org/10.1080/1536383X.2017.1373097

FULLERENES, NANOTUBES AND CARBON NANOSTRUCTURES
2017, VOL. 25, NO. 11, 642–645
https://doi.org/10.1080/1536383X.2017.1373097

Taylor & Francis
Taylor & Francis Group

A facile method for fabrication of large area graphene nanostructures

Cihan Kuru[a] and Sungho Jin[b]

[a]Department of Metallurgical and Materials Engineering, Bilecik Seyh Edebali University, Bilecik, Turkey; [b]Department of Mechanical and Aerospace Engineering, University of California-San Diego, La Jolla, CA, USA

ABSTRACT
In this study, we introduce a novel method to produce large area interconnected graphene nanostructures. A single layer CVD (Chemical Vapor Deposition) grown graphene was nanostructured by employing dewetted Ni thin film as an etching mask for the underlying graphene. As a result, a network of graphene nanostructures with irregular shapes and widths down to 10 nm is obtained. The FET (field effect transistor) devices fabricated employing the nanostructured graphene as channel material exhibit increased on/off current ratio compared to pristine graphene indicating a slight band gap opening due to the quantum confinement effect in such narrow graphene nanostructures. This technique can be useful for the large scale fabrication of graphene based electronic devices such as FETs and sensors.

ARTICLE HISTORY
Received 12 June 2017
Revised 1 August 2017
Accepted 25 August 2017

KEYWORDS
Nanostructured graphene; dewetting; nickel; field effect transistor; band gap

1. Introduction

Graphene, two dimensional hexagonally arranged carbon atoms, has received tremendous attention owing to its fascinating electronic, optical and mechanical properties.[1–4] High carrier mobilities have been observed in graphene, which makes it highly desirable for high speed electronics.[5–7] However, semimetallic nature of graphene hinders its application to digital devices since such a graphene device have small on/off current ratio.[8] One way to circumvent this problem is to fabricate narrow graphene nanostructures such as graphene nanoribbon or nanomesh, where quantum confinement of charge carriers leads to formation of a band gap.[9] Furthermore, graphene nanostructures is attractive for biological and gas sensing applications because nanostructured graphene shows higher sensitivity compared to its pristine counterpart.[10–13] To date, several methods have been reported for the fabrication of graphene nanostructures.[14–18] Most of these include lithography processes, which are complicated, expensive and incompatible with mass production.

Here, we present a simple and scalable method to fabricate graphene nanostructures. The dewetting of Ni thin film deposited on graphene with annealing provides an etching mask for the nanostructuring of graphene. We optimized the annealing temperature and time for the desired degree of dewetting. As the final product, a continuous network of graphene nanostructures is obtained. We investigated the structural properties of the nanostructured graphene by Raman spectroscopy and studied the transport properties by fabricating FET devices.

2. Experimental

CVD grown graphene on copper, purchased from ACS Materials, was transferred onto SiO_2 coated high doped Si substrates by well known PMMA (Poly(methyl methacrylate)) transfer method.[19] The fabrication procedure of the nanostructured graphene is schematically shown in Figure 1. After transferring graphene onto SiO_2 coated Si substrate, 5 nm thick Ni film was deposited on graphene by Temescal electron beam evaporator, where the thickness was monitored by a quartz crystal microbalance thickness sensor. Then, Ni/graphene film was annealed at 300°C in a tube furnace (Lindberg Mini Tube Furnace), which was kept under a constant flow of 5% H_2/N_2 mixture. The annealing process led to formation of interconnected Ni nanostructures, which serve as an etching mask for graphene. Next, uncovered regions of graphene were removed by O_2 plasma etching at 30 W RF (radio frequency) power for 40s using a Trion reactive ion etching system. Then, the samples were placed in concentrated nitric acid solution for 1 hour to remove the dewetted Ni film, followed by cleaning in deionized water for 2 hours. Subsequently, the samples were subjected to a post annealing process at 400°C in N_2 atmosphere in order to remove residual nitric acid molecules. The FET devices were constructed by photolithography, following evaporation of Ti/Au (10/100 nm) electrodes and lift off process. A second photolithography step combined with O_2 plasma etching was performed to define a channel with a length and width of 5 μm and 10 μm, respectively. Raman spectroscopy measurements were carried out by Renishaw RM1000 with a wavelength of 514 nm. Scanning electron microscopy (SEM) images were taken with FEI SFEG UHR SEM (Schottky Field Emitter Gun Ultra High Resolution Scanning Electron Microscope). The transport measurements were conducted at room temperature with Agilent B1500 semiconductor device analyzer.

CONTACT Cihan Kuru ✉ cihan.kuru@bilecik.edu.tr Bilecik Seyh Edebali Universitesi, Muhendislik Fakultesi, 11230, Bilecik, Turkey.

Color versions of one or more of the figures in the article can be found online at www.tandfonline.com/lfnn.

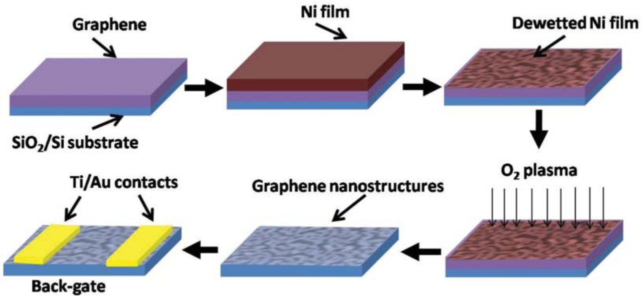

Figure 1. Schematic depiction of the fabrication procedure of the nanostructured graphene FET devices.

3. Results and discussion

When metal thin films are heated, a structural change called dewetting occurs in order to minimize the free energy of the film/substrate system.[20] Dewetting is considered to be a two step process: void nucleation and following void growth.[21] Void nucleation is induced by defects, pinholes, gas bubbles and grain boundary triple points.[21] In this study, we took advantage of dewetting of Ni thin film as a self assembly process to form a network of Ni nanostructures, which was then employed as an etching template for the underlying graphene. Ni was chosen as the dewetting material for two reasons: First, we could deposit ultra-thin Ni film with high degree of thickness control. Second, Ni thin film does not require high temperature for dewetting.

Figure 2 shows the SEM images of 5 nm thick Ni film on graphene, which was annealed at 300°C under 5% H_2/N_2 flow for different time durations. As-deposited Ni film is continuous (Figure 2a). Void formation is apparent in the Ni film annealed for 5 minutes (Figure 2b). With further annealing, voids grow into a porous network of Ni nanostructures (Figure 2c). Note that the brighter regions in the image correspond to Ni. When the sample is annealed longer, discrete Ni islands are constructed (Figure 2d). Since any charge transport device needs to be continuous, we optimized the annealing temperature and time to attain a continuous network of Ni nanostructures. As seen in the SEM images, annealing of the 5 nm thick Ni film at 300°C for 10 minutes is the optimum condition for the desired degree of dewetting. We have found that H_2 is crucial for the dewetting of Ni films on graphene because no dewetting behavior could be observed for the samples annealed in pure N_2 atmosphere. This can be attributed to the formation of nickel hydride compounds in the presence of H_2, which leads to an increase in the free energy of the Ni/graphene system promoting the dewetting of the Ni film.[22]

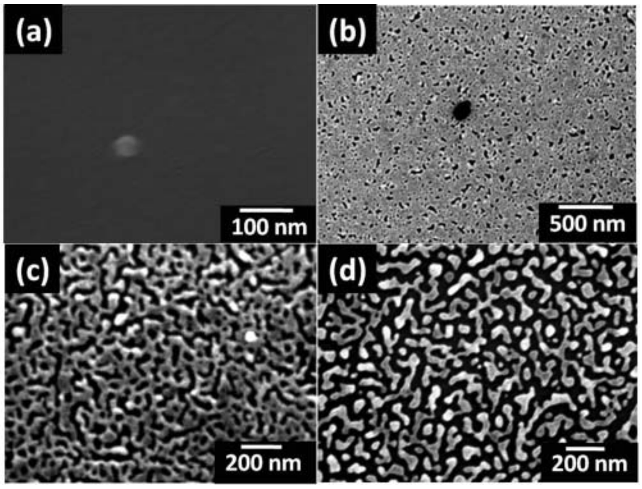

Figure 2. SEM images of (a) As-deposited 5 nm thick Ni film. (b) 5 nm thick Ni film annealed at 300°C for 5 minutes. (c) 5 nm thick Ni film annealed at 300°C for 10 minutes. (d) 5 nm thick Ni film annealed at 300°C for 20 minutes.

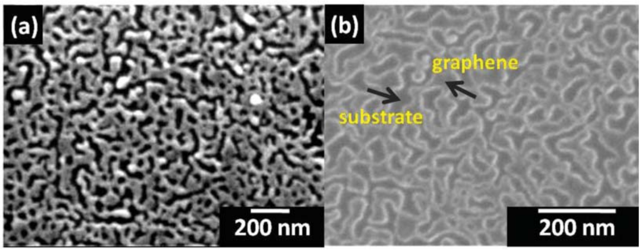

Figure 3. SEM images of the (a) dewetted 5 nm thick Ni film and (b) corresponding graphene nanostructures.

The SEM images of the dewetted Ni film used as etching mask and the corresponding graphene nanostructures are exhibited in Figure 3. In Figure 3b, the slightly lighter regions represent the graphene nanostructures. The nanostructured graphene has a similar construction to the dewetted Ni film showing that the pattern was successfully transferred to graphene after the O_2 plasma etching and removal of the Ni film. The resulting graphene nanostructures are irregular features whose widths roughly range from 10 nm to 50 nm. We were able to fabricate graphene nanostructures over 1 cm^2 area. Larger area nanostructuring should also be possible when a larger tube furnace is used for the dewetting.

We conducted Raman spectroscopy measurements to investigate the structural properties of the graphene samples. Figure 4 depicts the Raman spectra of the pristine and nanostructured graphene, in which the main peaks of graphene are observed for both samples. The intensity of D peak is associated with the degree of disorder in graphene.[23] The intensity ratio of D peak to G peak (I_D/I_G) can be used to compare the defect density in graphene.[23] There is a dramatic increase in I_D/I_G after the nanostructuring of the graphene sample (from 0.09 to 0.95), resulted from the formation of edge defects after the oxygen plasma etching process.[24] Moreover, a new peak denoted as D'

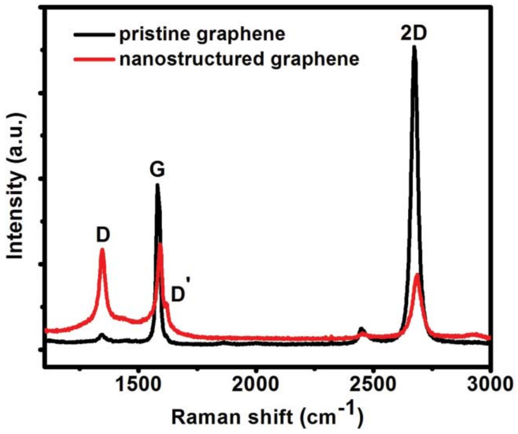

Figure 4. Raman spectra of the pristine and nanostructured graphene.

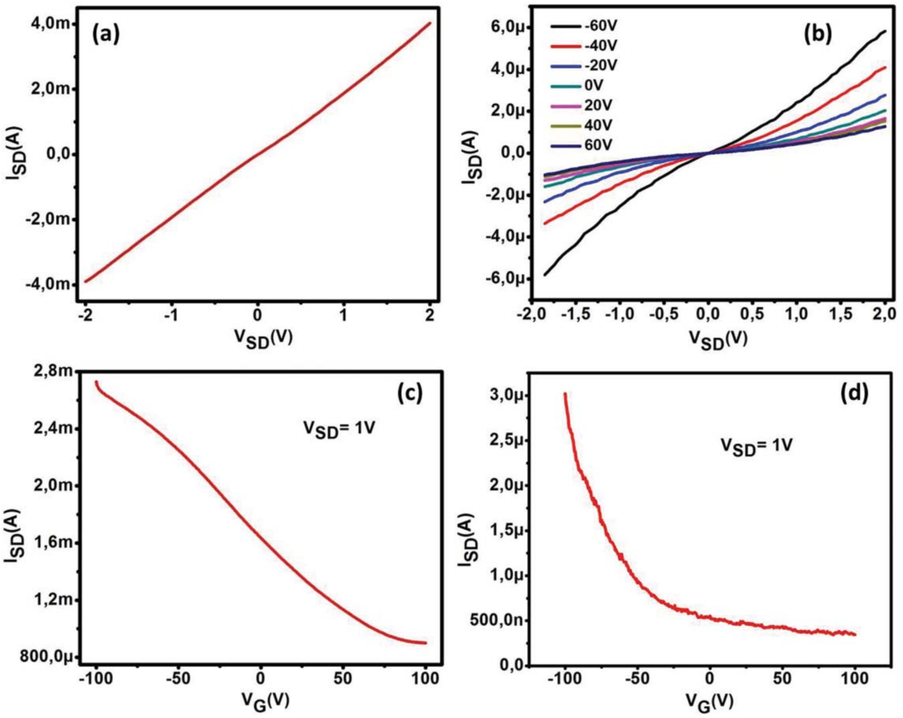

Figure 5. (a) Source-drain current versus source-drain voltage plot of the pristine graphene. (b) Source-drain current versus source-drain voltage plot of the nanostructured graphene under varying gate voltages. (c) Source-drain current versus gate voltage plot of the pristine graphene. (d) Source-drain current versus gate voltage plot of the nanostructured graphene.

has emerged at a frequency of $\sim$1618 cm^{-1}, which is only activated with excess number of disorder.[25] Furthermore, we observed an upshift in the positions of the G and 2D peak. The upshift suggests hole doping in graphene, which was emanated from the oxidation of graphene edges during the oxygen plasma etching as well as nitric acid exposure.[26]

We fabricated FET devices employing both pristine and nanostructured graphene as the channel materials. Heavily doped Si back-gate and 300 nm thick thermally grown SiO_2 gate dielectric was used to apply a gate voltage (V_G) to the devices. Figure 5a shows the current-voltage (I-V) characteristics of the pristine graphene device. The measured source-drain current (I_{SD}) linearly changes as the source-drain voltage (V_{SD}) is swept from -2 V to $+2$ V implying the metallic nature of the pristine graphene sample.[27] We measured the I-V behavior of the nanostructured graphene device in the same V_{SD} range under varying V_G, in which the nanostructured graphene device exhibits a non-linear I-V relationship (Figure 5b). Such a non-linear behavior points out the existence of a Schottky barrier between the contacts and the channel, which results from semiconducting nature of the nanostructured graphene.[17] The semiconducting nature of the nanostructured graphene was also evidenced by measuring the I_{SD} as a function of V_G. The I_{SD} was measured at constant V_{SD} of 1V while V_G was swept from -100 V to $+100$ V. The pristine graphene FET device has an on/off ratio of 3 (Figure 5c), which is typical for unpatterned single layer graphene.[28,29[For the device comprising nanostructured graphene, we observed an increased on/off current ratio of 9 (Figure 5d). The on/off current ratio exponentially scales with band gap in accordance with $I_{on} / I_{off} \approx \exp\left(E_g / 2k_bT\right)$, where E_g is the band gap energy, k_b is the Boltzmann constant and T is absolute temperature.[14] Hence, an increased on/off current ratio signifies a band gap opening for the nanostructured graphene. The quantum confinement of charge carriers in the narrow graphene nanostructures causes the emergence of the band gap, which scales inverse linearly with the widths of the graphene nanostructures.[15] The on current value of the nanostructured graphene device is three orders of magnitude lower than the pristine graphene one. This can be explained by the formation of edge defects after nanostructuring of graphene, which act as scattering centers for charge carriers impeding the conductivity.[30] In addition, the nanostructured graphene FET device shows a typical p-type transport behavior, consistent with the Raman spectroscopy measurements.

The nanostructured graphene is also preferable for sensing applications. It was reported that nanopatterned graphene was more sensitivity to toxic gas molecules than unpatterned graphene.[10,11] The enhanced sensitivity mainly arises from the presence of large amount of edge defects, which have higher activity for the adsorption of gas molecules.[31] Moreover, the opening of a band gap in such graphene nanostructures results in a reduced carrier concentration, which enables larger conductance modulation with the adsorption of sensed gas molecules.[11]

4. Conclusion

In conclusion, we have developed a facile method for the scalable and low cost fabrication of graphene nanostructures. This method allows the fabrication of graphene nanostructures with widths as low as 10 nm. The nanostructured graphene shows semiconducting behavior and possesses abundance of edge defects indicated by electrical transport and Raman spectroscopy measurements, respectively. Such nanostructured graphene holds a great promise for applications in logic devices and sensors.

Funding

This work was supported by Iwana Endowed Fund at UC San Diego.

References

[1] Novoselov, K. S.; Geim, A. K.; Morozov, S.; Jiang, D.; Katsnelson, M.; Grigorieva, I.; Dubonos, S.; Firsov, A. Two-Dimensional Gas of Massless Dirac Fermions in Graphene. *Nature* **2005**, *438*(7065), 197–200. doi:10.1038/nature04233.

[2] Neto, A. C.; Guinea, F.; Peres, N. M.; Novoselov, K. S.; Geim, A. K. The Electronic Properties of Graphene. *Rev. Mod. Phys.* **2009**, *81*(1), 109. doi:10.1103/RevModPhys.81.109.

[3] Nair, R. R.; Blake, P.; Grigorenko, A. N.; Novoselov, K. S.; Booth, T. J.; Stauber, T.; Peres, N. M.; Geim, A. K. Fine Structure Constant Defines Visual Transparency of Graphene. *Science* **2008**, *320*(5881), 1308–1308. doi:10.1126/science.1156965.

[4] Frank, I. W.; Tanenbaum, D. M.; Van der Zande, A. M.; McEuen, P. L. Mechanical Properties of Suspended Graphene Sheets. *Journal of Vacuum Science & Technology B: Microelectronics and Nanometer Structures Processing, Measurement, and Phenomena* **2007**, *25*(6), 2558–2561. doi:10.1116/1.2789446.

[5] Bolotin, K. I.; Sikes, K. J.; Jiang, Z.; Klima, M.; Fudenberg, G.; Hone, J.; Kim, P.; Stormer, H. L. Ultrahigh Electron Mobility in Suspended Graphene. *Solid State Commun.* **2008**, *146*(9), 351–355. doi:10.1016/j.ssc.2008.02.024.

[6] Dean, C. R.; et al. Boron Nitride Substrates for High-Quality Graphene Electronics. *Nat. Nanotechnol.* **2010**, *5*(10), 722–726. doi:10.1038/nnano.2010.172.

[7] Kim, S.; Nah, J.; Jo, I.; Shahrjerdi, D.; Colombo, L.; Yao, Z.; Tutuc, E.; Banerjee, S. K. Realization of a High Mobility Dual-Gated Graphene Field-Effect Transistor with Al2O3 Dielectric. *Appl. Phys. Lett.* **2009**, *94*(6), 062107. doi:10.1063/1.3077021.

[8] Schwierz, F. Graphene Transistors. *Nat. Nanotechnol.* **2010**, *5*(7), 487–496. doi:10.1038/nnano.2010.89.

[9] Berger, C.; et al. Electronic Confinement and Coherence in Patterned Epitaxial Graphene. *Science* **2006**, *312*(5777), 1191–1196. doi:10.1126/science.1125925.

[10] Paul, R. K.; Badhulika, S.; Saucedo, N. M.; Mulchandani, A. Graphene Nanomesh as Highly Sensitive Chemiresistor Gas Sensor. *Anal. Chem.* **2012**, *84*(19), 8171–8178. doi:10.1021/ac3012895.

[11] Abbas, A. N.; Liu, G.; Liu, B.; Zhang, L.; Liu, H.; Ohlberg, D.; Wu, W.; Zhou, C. Patterning, Characterization, and Chemical Sensing Applications of Graphene Nanoribbon Arrays Down to 5 Nm Using Helium Ion Beam Lithography. *ACS Nano* **2014**, *8*(2), 1538–1546. doi:10.1021/nn405759v.

[12] Zribi, B.; Castro-Arias, J. M.; Decanini, D.; Gogneau, N.; Dragoe, D.; Cattoni, A.; Ouerghi, A.; Korri-Youssoufi, H.; Haghiri-Gosnet, A. M. Large Area Graphene Nanomesh: An Artificial Platform for Edge-Electrochemical Biosensing at the Sub-Attomolar Level. *Nanoscale* **2016**, *8*(34), 15479–15485. doi:10.1039/C6NR04289A.

[13] Pak, Y.; et al. Palladium-Decorated Hydrogen-Gas Sensors Using Periodically Aligned Graphene Nanoribbons. *ACS Applied Materials & Interfaces* **2014**, *6*(15), 13293–13298. doi:10.1021/am503105s.

[14] Son, J. G.; Son, M.; Moon, K. J.; Lee, B. H.; Myoung, J. M.; Strano, M. S.; Ham, M. H.; Ross, C. A. Sub−10 nm Graphene Nanoribbon Array Field−Effect Transistors Fabricated by Block Copolymer Lithography. *Adv. Mater.* **2013**, *25*(34), 4723–4728. doi:10.1002/adma.201300813 10.1002/adma.201370213.

[15] Liang, X.; Jung, Y. S.; Wu, S.; Ismach, A.; Olynick, D. L.; Cabrini, S.; Bokor, J. Formation of Bandgap and Subbands in Graphene Nanomeshes with Sub-10 Nm Ribbon Width Fabricated via Nanoimprint Lithography. *Nano Lett.* **2010**, *10*(7), 2454–2460. doi:10.1021/nl100750v.

[16] Zeng, Z.; Huang, X.; Yin, Z.; Li, H.; Chen, Y.; Li, H.; Zhang, Q.; Ma, J.; Boey, F.; Zhang, H. Fabrication of Graphene Nanomesh by Using an Anodic Aluminum Oxide Membrane as a Template. *Adv. Mater.* **2012**, *24*(30), 4138–4142. doi:10.1002/adma.201104281.

[17] Stampfer, C.; Güttinger, J.; Hellmüller, S.; Molitor, F.; Ensslin, K.; Ihn, T. Energy Gaps in Etched Graphene Nanoribbons. *Phys. Rev. Lett.* **2009**, *102*(5), 056403. doi:10.1103/PhysRevLett.102.056403.

[18] Bell, D. C.; Lemme, M. C.; Stern, L. A.; Williams, J. R.; Marcus, C. M. Precision Cutting and Patterning of Graphene with Helium Ions. *Nanotechnology* **2009**, *20*(45), 455301. doi:10.1088/0957-4484/20/45/455301.

[19] Suk, J. W.; Kitt, A.; Magnuson, C. W.; Hao, Y.; Ahmed, S.; An, J.; Swan, A. K.; Goldberg, B. B.; Ruoff, R. S. Transfer of CVD-Grown Monolayer Graphene onto Arbitrary Substrates. *ACS Nano* **2011**, *5*(9), 6916–6924. doi:10.1021/nn201207c.

[20] Thompson, C. V. Solid-State Dewetting of Thin Films. *Annu. Rev. Mater. Res.* **2012**, *42*, 399–434. doi:10.1146/annurev-matsci-070511-155048.

[21] Petersen, J.; Mayr, S. G. Dewetting of Ni and NiAg Solid thin Films and Formation of Nanowires on Ripple Patterned Substrates. *J. Appl. Phys.* **2008**, *103*(2), 023520. doi:10.1063/1.2832758.

[22] Geissler, A.; He, M.; Benoit, J. M.; Petit, P. Effect of Hydrogen Pressure on the Size of Nickel Nanoparticles Formed During Dewetting and Reduction of Thin Nickel Films. *The Journal of Physical Chemistry C* **2009**, *114*(1), 89–92. doi:10.1021/jp908427r.

[23] Ferrari, A. C. Raman Spectroscopy of Graphene and Graphite: Disorder, Electron–Phonon Coupling, Doping and Nonadiabatic Effects. *Solid State Commun.* **2007**, *143*(1), 47–57. doi:10.1016/j.ssc.2007.03.052.

[24] Shi, Z.; Yang, R.; Zhang, L.; Wang, Y.; Liu, D.; Shi, D.; Wang, E.; Zhang, G. Patterning Graphene with Zigzag Edges by Self−Aligned Anisotropic Etching. *Adv. Mater.* **2011**, *23*(27), 3061–3065. doi:10.1002/adma.201100633.

[25] Cançado, L. G.; Jorio, A.; Ferreira, E. M.; Stavale, F.; Achete, C. A.; Capaz, R. B.; Moutinho, M. V. O.; Lombardo, A.; Kulmala, T. S.; Ferrari, A. C. Quantifying Defects in Graphene via Raman Spectroscopy at Different Excitation Energies. *Nano Lett.* **2011**, *11*(8), 3190–3196. doi:10.1021/nl201432g.

[26] Das, A.; et al. Monitoring Dopants by Raman Scattering in an Electrochemically Top-Gated Graphene Transistor. *Nat. Nanotechnol.* **2008**, *3*(4), 210–215. doi:10.1038/nnano.2008.67.

[27] Novoselov, K. S.; Geim, A. K.; Morozov, S. V.; Jiang, D.; Zhang, Y.; Dubonos, S. V.; Grigorieva, I. V.; Firsov, A. A. Electric Field Effect in Atomically Thin Carbon Films. **2004**, *Science 306*(5696), 666–669. doi:10.1126/science.1102896.

[28] Lin, Y. M.; Dimitrakopoulos, C.; Jenkins, K. A.; Farmer, D. B.; Chiu, H. Y.; Grill, A.; Avouris, P. 100-GHz Transistors from Wafer-Scale Epitaxial Graphene. *Science* **2010**, *327*(5966), 662–662. doi:10.1126/science.1184289.

[29] Wang, M.; et al. A Platform for Large−Scale Graphene Electronics–CVD Growth of Single−Layer Graphene on CVD−Grown Hexagonal Boron Nitride. *Adv. Mater.* **2013**, *25*(19), 2746–2752. doi:10.4028/www.scientific.net/AMR.690-693.2746 10.1002/adma.201204904.

[30] Jia, X.; Campos-Delgado, J.; Terrones, M.; Meunier, V.; Dresselhaus, M. S. Graphene Edges: A Review of Their Fabrication and Characterization. *Nanoscale* **2011**, *3*(1), 86–95. doi:10.1039/C0NR00600A.

[31] Huang, B.; Li, Z.; Liu, Z.; Zhou, G.; Hao, S.; Wu, J.; Gu, B. L.; Duan, W. Adsorption of Gas Molecules on Graphene Nanoribbons and its Implication for Nanoscale Molecule Sensor. *The Journal of Physical Chemistry C* **2008**, *112*(35), 13442–13446. doi:10.1021/jp8021024.